BASIC UNDERSTANDING FOR THE VARIOUS CAUSES OF QUENCH

D. Meidlinger*, CLASSE, Cornell University, Ithaca, NY, U.S.A.

Abstract

The maximum possible CW accelerating gradient in a superconducting cavity is often limited by a quench caused by a small defect on the RF surface. Sometimes the defect takes the form of a large (on the order of 100 μm) pit in the surface. In addition, the quench field for a pit is generally lower than for a normal-conducting defect with the same size. A brief survey of previous work and current theories on the nature and causes of quench is given, including recent theories on the quench mechanism of niobium pits.

INTRODUCTION

In this article, quench will be described in terms of the classical thermal model [1] (see Fig. 1): the high power dissipation in a small, lossy defect on the RF surface causes the temperature of the surrounding superconductor to rise above the transition temperature T_C. At this point, the normal-conducting region grows rapidly (≈10's of μs) until the entire stored energy has dissipated away.

Defects may be introduced at various stages of cavity fabrication. Fig. 3 shows examples of an inclusion [2] containing S, Ca, Cl, and K (quench field = 10.7 MV/m), a Nb protrusion (quench field = 18 MV/m), a weld hole [2], and a chemical drying stain [2] (quench field 3.4 MV/m). Fig. 4 shows examples of a Nb pit [3] (quench field = 1200 Oe) and copper particle [3] (no quench) with plots of the preheating measured during tests at Cornell. The ohmic losses of a simple normal-conducting defect such as the copper particle are clearly observed, whereas the preheating of the Nb pit indicates a more complicated dependence on the surface magnetic field level. These examples demonstrate how the measured preheating from resistive thermometry can detect different types of detects.

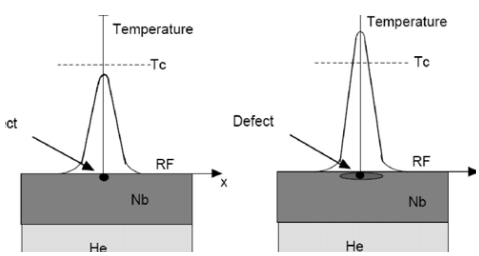

Figure 1: Classical model of thermal breakdown.

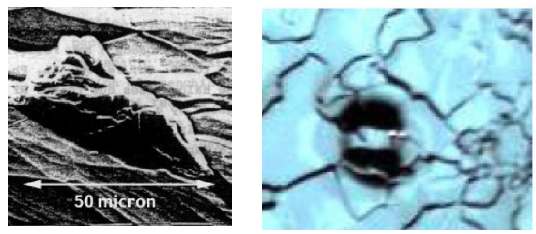

(a) inclusion (b) Nb protrusion

(c) weld hole (d) stain defect

Figure 2: Examples of quench-limiting defects.

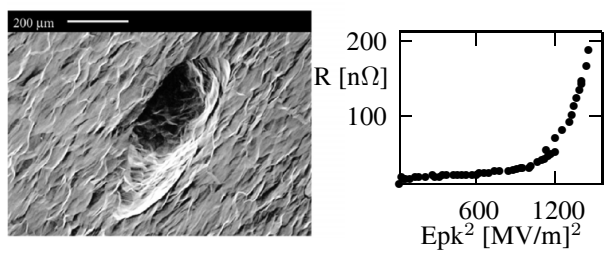

(a) Nb pit (b) pit preheating

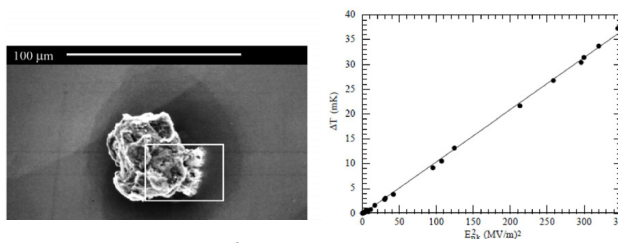

(c) copper defect (d) copper preheating

Figure 3: Measured preheating for a Nb pit and a copper particle.

The most simple model of thermal breakdown assumes that all material properties are constants, independent of temperature and field level and that the defect is a normal conducting hemisphere [1]. Such a simple model has the virtue of being analytically tractable. It is to be expected

* djm226@cornell.edu

that the numerical predictions will not be very accurate; nevertheless, the main points are present in the analytic solution for the surface magnetic field $H_{\rm max}$ at quench:

$$H_{\rm max} = \sqrt{\frac{4\kappa(T_{\rm C} - T_{\rm b})}{aR_{\rm n}}} \qquad (1)$$

where κ is the thermal conductivity of niobium, $T_{\rm b}$ is the helium bath temperature, a is the defect radius, and $R_{\rm n}$ is the normal resistance of the defect. This expression is consistent with the following experimental observations:

1. normal-conducting defects of smaller size and resistance result in higher quench fields;
2. lowering the bath temperature increases the quench field; and
3. increasing Nb thermal conductivity results in higher quench fields.

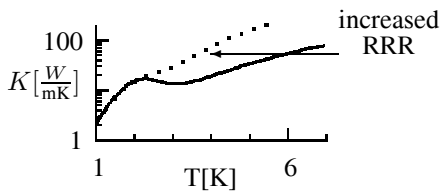

Figure 4: Increasing Nb purity increases thermal conductivity.

The thermal conductivity of niobium does, in fact, depend on temperature, and this dependence is plotted in Fig. 4. Historically, the best means of attaining higher fields before quenching has been to increase the RRR of the niobium. The increase in thermal conductivity occurs at the higher temperatures (≈6 K) that are typical surrounding a defect. The thermal conductivity also has a dependence on grain size, as this effectively determines the mean free path for phonon scattering. The so called "phonon peak" (see Fig. 5) does not generally help in increasing the quench field as the peak occurs at lower temperatures than is typical in the vicinity of a defect; however, as we push the state of the art to higher quench fields and approach the limit of a defect-free cavity, $T_{\rm C}$ will decrease at these higher magnetic fields. The presence of the phonon peak would then be more vital.

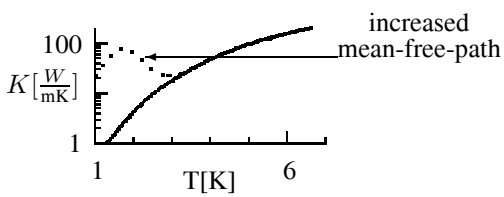

Figure 5: Larger grain sizes produce a "phonon peak" in the thermal conductivity at low temperature.

For accurate quantitative predictions of quench fields, numerical heat transfer simulations are required that take into account the dependence of the BCS resistance on temperature, field level, and material properties such as the mean free path; also, the temperature dependence of the thermal conductivity must be considered. Fig. 6 shows the results [4] of such simulations used for predicting the quench field for various RRR in niobium.

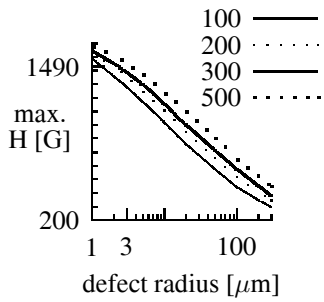

Figure 6: Numerical calculations of quench fields for various RRR.

These results predict that for a cavity to quench at a magnetic field greater than 1490 Oe (corresponding to 35 MV/m for the TESLA geometry), a 10 mΩ defect must have a radius less than 3μm. This is at or below the resolution of current optical inspection systems; therefore, normal-conducting defects for high-gradient structures may be difficult to observe directly. This conclusion may be too restrictive since the assumption that all defects can be approximated as round discs with a surface resistance of ≈10 mΩ is not generally valid. Some defects such as niobium pits or protrusions may have a much smaller effective resistance; nevertheless, all is not lost, since the defect properties can be inferred from a combination of RF and thermometric measurements.

THERMOMETRIC MEASUREMENTS

The cavity field level just prior to quench can be measured; however, this information is not sufficient to uniquely determine the properties of the defect even for the simple model of a circular, normal-conducting defect. In this model, the defect is characterized by two properties: its radius and resistance. The quench field is only one value; additional information is required. To illustrate this point, consider the example shown in Fig. 7. Heat transfer simulations were done for two defects: a 15μm defect with a resistance of 10 mΩ and a 150 μm defect with a resistance of 1 mΩ [5]. The plot shows the temperature just outside of the defects is the same at transition, so both defects result in the same quench field.

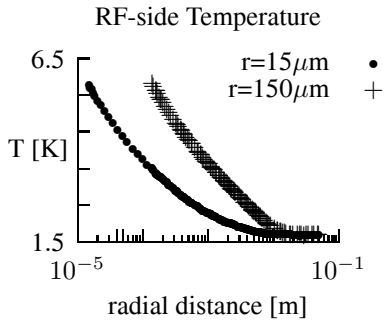

Figure 7: Calculated temperature profile on the RF surface near the defect.

The total heat produced by the 150 μm defect is the greater of the two, but the side-heating is the same for both defects. The side-heating is the rate of heat transfer through the sides of an imaginary cylinder which extends down from the defect to the helium side of the niobium wall. It is generally found that the side heating determines the quench field [4] and that the fraction of the total heat which passes through the sides is equal to the ratio of the area of the cylinder wall to the the total area of the wall and bottom. From this geometric fact, the simple inverse scaling relationship between defect size and resistance can be deduced. Since the larger defect dissipates more heat, it is not entirely surprising that the simulation results [5] shown in Fig. 8 predict the temperature of the helium-side of the wall to be larger for the larger defect. The wall temperature is then the additional information required to characterize a defect with the circular model. By combining the measured quench field and wall temperature with numerical simulations, the defect size and resistance can be inferred.

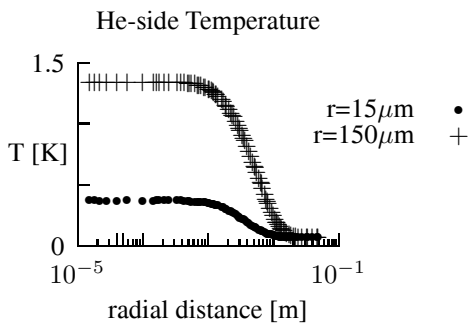

Figure 8: Calculated temperature profile near the defect on the Helium side of the wall.

PITS AND PROTRUSIONS

Why do large ($\approx$100μm) pits cause quench at higher fields than would be expected for normal conducting defects of the same size? Why would the preheating observed, as in Fig. 3b, be different from the case of simple ohmic losses in a normal conducting particle? The obvious answer is that only a small portion of the pit goes normal conducting. It is encouraging that thermometric measurements of the type described in the previous section are consistent with this model. Fig. 9 shows two pictures of the same pit found in a single cell cavity tested at Cornell [5].

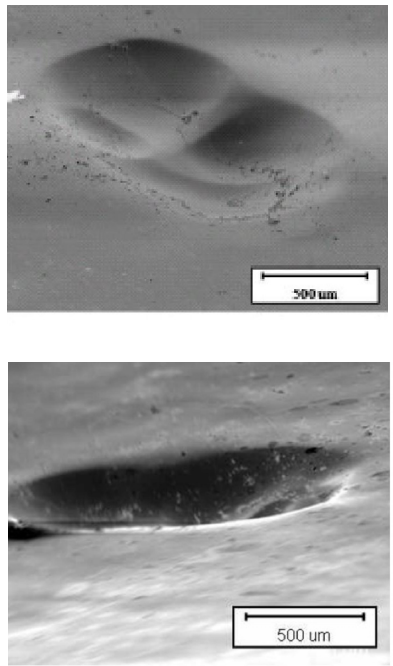

Figure 9: Two views with scanning electron microscopy of the same Nb pit.

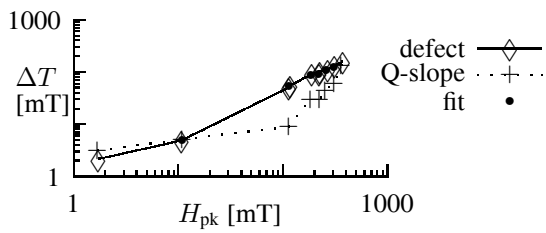

(a) pit preheating

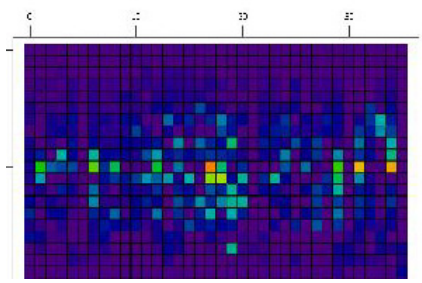

(b) temperature map

Figure 10: Measured preheating at the pit in the presence of high-field Q-slope.

This cavity did not undergo baking and subsequently there was a strong Q-slope observed at high fields. Fig. 10b shows one of the temperature maps taken in the Q-slope

region. The preheating measured at the location of the red square in the middle of the temperature map indicated that additional heating above what is expected for Q-slope was present. The temperature rise at this location is shown in Fig. 10a. By combining ohmic losses with the Q-slope heating measured in the area surrounding the defect, a close fit to the measured preheating curve was obtained. The resistance corresponding to the ohmic losses for this close fit is 0.5 mΩ to 2 mΩ. Combining this information with the measured quench field led to an estimate of the area of the normal conducting defect of 40 to 50 μm. This area is much smaller than the size of the actual pit observed with electron microscopy.

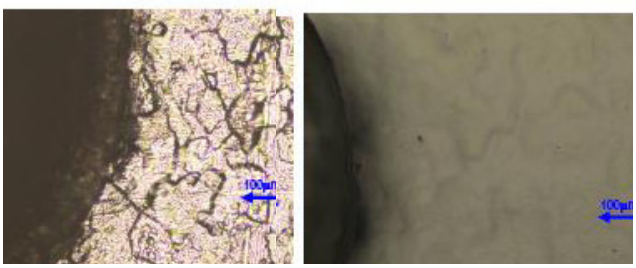

(a) before EP (b) after EP

Figure 11: Electropolishing can sharpen the edges of pits.

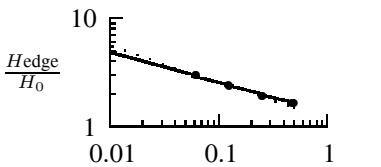

(a) calculated H-enhancement

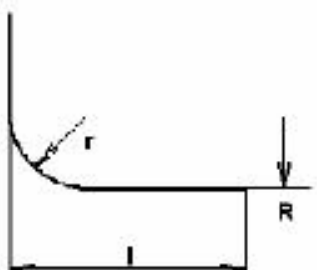

(b) model geometry

Figure 12: Predictions of field enhancement from RF simulations.

The size estimates of the normal-conducting region are comparable to the area of the edges around the pit, which is likely the normal conducting area due to magnetic field enhancement. Tests on the effects of electropolishing on artificially produced pits [6] indicate that electropolishing can sharpen the edges of the pits (see Fig. 11). The results of RF simulations [7], shown in Fig. 12a, indicate that the edge can locally enhance the magnetic field by as much as a factor of four. Electropolishing has also been shown to increase the size of pits. [6] Fig.13 shows pictures of an artificially produced pit before and after having 30 μm removed via buffered chemical polish and 120 μm removed by electropolishing [8].

(a) before EP (b) after EP

Figure 13: 120 μm EP Increases Pit Size.

Sharpening the edges of pits and increasing the pit size both tend to decrease the quench field. In order to better understand what role the pit geometry has in heat transfer and in determining the quench field, heat transfer simulations were done at Cornell which used a ring type defect shape as opposed to a solid disk [9]. The ring in Fig. 14b is meant to represent the normal-conducting edge of a pit.

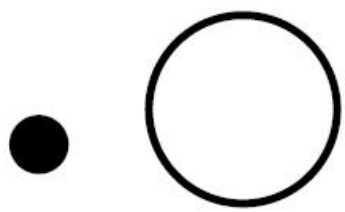

(a) disk defect (b) ring defect

Figure 14: A ring is used in heat transfer calculations to model the normal-conducting edge of a pit.

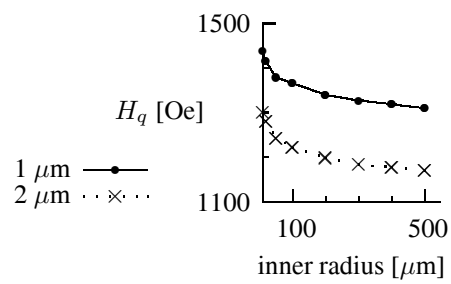

Figure 15: The dependence of quench field on ring radius is measured for two different ring widths.

This model ignores certain features of real pits such as the non-circular shape, the variation in edge sharpness, and

the depth profile to name a few, but even this simple model already has three free parameters (one more than the solid disc-type defect): the inner radius, the outer radius, and the resistance. The dependence of the quench field on pit size was determined by fixing the width of the ring at 1 μm and varying the inner radius. The results are shown in Fig. 15. It is seen that larger ring diameters lower the quench field. The physical reason for this is simply that the total normal-conducting area increases linearly with the radius. It is also seen that the quench field drops rapidly for radii less than approximately 100 μm.

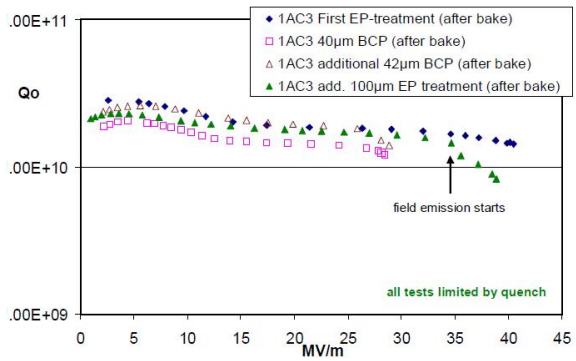

Figure 16: Vertical tests at DESY show BCP lowering the quench field.

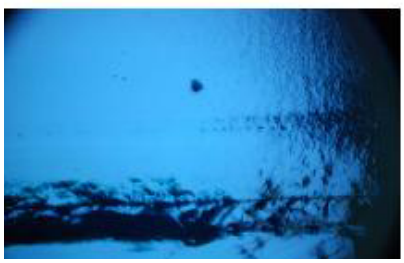

(a) 700 μm defect , quench at 20 MV/m

(b) 1mm defect, maximum E_a =39 MV/m, no quench

Figure 17: Large pits do not always result in low quench fields.

OPEN QUESTIONS

Which is more important: the diameter or the edge? Why is the maximum accelerating field at quench for TESLA-style cavities with pits approximately 30 MV/m? H_{pk} =1235 Oe at this field level, which is close to the quench fields shown in Fig. 15 for typical pit properties. While there is a rapid drop in quench field for radii less than 100 μm, the quench field is also very dependent on the width of the normal-conducting ring. For example, one could imagine a heavy electropolish increasing the size of a pit (as depicted in the pictures of Fig. 13) which lowers the quench field; however, if the electropolishing also changed the edge properties such that the normal-conducting width decreases from 2 μm to 1 μm, then Fig. 15 shows that the quench field would actually increase. Even the simple model of the ring-type defect illustrates the need for basic information about the pit geometry to accurately model the heat transfer and predict quench field. Large pits don't always result in low quench fields. Fig. 17 shows pits found in two different cavities tested at FNAL [10]. One cavity had a 700 μm pit and quenched at E_a <20 MV/m, while the other cavity had a 1 mm pit and reached E_a=39 MV/m without quench. Another open question relates to the observed difference in quench field between cavities treated with a buffered chemical polish (BCP) and cavities electropolished (EP). Fig. 16 shows the results of multiple tests on the same 9-cell cavity tested at DESY [11]. The vertical tests repeatedly showed the cavity quenching at 10 MV/m lower when BCP was used. It is still true that BCP cavities quench at lower fields than EP cavities when a larger sample population is studied. Fig. 18 shows the distribution of measured quench fields for 5-cell CEBAF cavities prepared with BCP and for 9-cell cavities prepared with EP at DESY. It is seen that the BCP cavities quench at a most probable field of 14 to 15 MV/m, whereas the EP cavities most probable quench field is 30 to 35 MV/m. A statistical analysis was done at Cornell to determine what probability distribution for defect size would produce a quench field distribution which closely fits the measurements [4]. The results shown in Fig. 19 indicate that the BCP cavities have much larger defects ($\approx$50μm) than those in EP cavities ($\approx$2μm). What about the chemical treatment affects the defect size? The large steps at BCP grain boundaries could possibly trap large defects, but there could also be an additional effect of field enhancement at the grain boundary. A normal-conducting particle located at a grain boundary would experience more losses due to the increased surface current from field enhancement. The heat transfer simulations used in the Cornell study assumed a constant defect resistance of 10 mΩ and did not take field enhancement at grain boundaries into account; therefore, any additional defect losses due to field enhancement would tend to increase the size of the constant resistance defect assumed in the model.

CONCLUSIONS

The thermal model is a reasonable description of the quench mechanism. The thermal model with ring-type defects helps explain why some pits quench and others do not. Thermometry is still key to understanding defects with quench fields at 35 MV/m and beyond, since the size of the heating region can be determined by thermometric mea-

surements of preheating. In this way, defects smaller than the resolution of optical inspection systems may be studied.

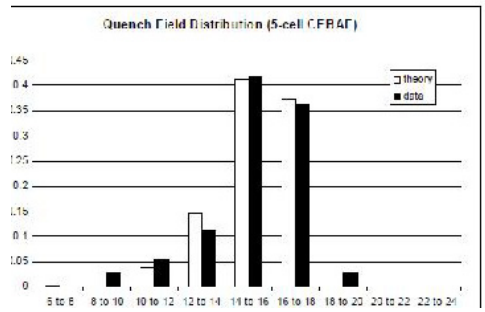

(a) CEBAF 5-cell quench fields

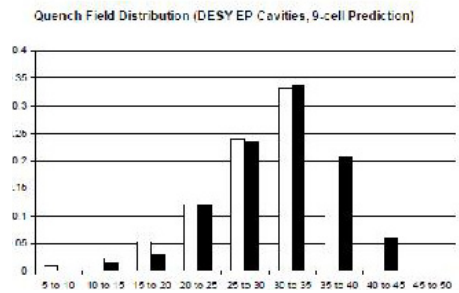

(b) DESY 9-cell quench fields

Figure 18: Classical model of thermal breakdown.

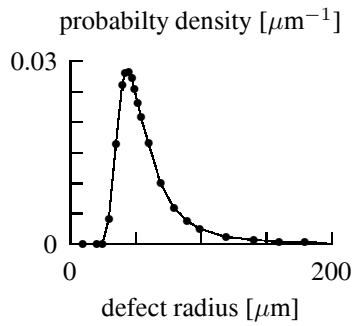

(a) CEBAF 5-cell probable defect size

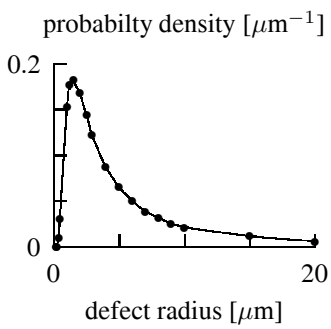

(b) DESY 9-cell probable defect size

Figure 19: Classical model of thermal breakdown.

REFERENCES

[1] H. Padamsee, J. Knobloch, and T. Hays, *RF Superconductivity for Accelerators*, Wiley and Sons,New York, 1998

[2] H.Piel, *Superconducting Cavities, CERN Accelerator School*, May-June 1988, CERN89-04, S. Turner(ed)(1989), p.149

[3] J. Knobloch, *Advanced Thermometry Studies of Superconducting Radio-Frequency Cavities*, PhD Thesis, Cornell University, Ithaca, 1997

[4] J. Wiener and H. Padamsee, *Thermal and Statistical Models for Quench in Superconducting Cavities*, TTC-Report 2008-08

[5] Y. Xie, H. Padamsee, and A. Romanenko, *Relationship Between Defects Pre-Heating and Defects Size*, this conference

[6] P. Michelato, *Evolution of Surface Defect During Niobium EP*, TTC meeting, Orsay, June 16-19, 2009

[7] V. Shemelin and H. Padamsee, *Magnetic Field Enhancement at Pits and Bumps on the Surface of Superconducting Cavities*, TTC-Report 2008-07

[8] F. Eozenou, *EP at Saclay: Last Results*, TTC meeting, Orsay, June 16-19, 2009

[9] Y. Xie, M. Liepe, and D. Meidlinger, *Thermal Modeling of Ring-Type Defects*, this conference

[10] S. Mishra, *ILC and SRF Program*, TTC meeting, Orsay, June 16-19, 2009

[11] D. Reschke, *Analysis of Quenches Using Temperature Mapping in 1.3 GHz Superconducting Cavities at DESY*, Proceedings of LINAC08, Victoria, BC, Canada